Biological Templated Synthesis of Water-Soluble Conductive Polymeric Nanowires

ARTICLE *in* NANO LETTERS · JANUARY 2008

Impact Factor: 13.59 · DOI: 10.1021/nl072134h · Source: PubMed

NANO LETTERS

2007
Vol. 7, No. 12
3729−3733

Biological Templated Synthesis of Water-Soluble Conductive Polymeric Nanowires

Zhongwei Niu,[†] Jie Liu,[‡] L. Andrew Lee,[†] Michael A. Bruckman,[†] Donggao Zhao,[§] Goutam Koley,*[,‡] and Qian Wang*[,†]

Department of Chemistry and Biochemistry and Nanocenter, University of South Carolina, 631 Sumter Street, Columbia, South Carolina 29208, Department of Electrical Engineering, University of South Carolina, 301 South Main Street, Columbia, South Carolina 29208, and The Electron Microscopy Centre, University of South Carolina, 715 Main Street, Columbia, South Carolina 29208

Received August 23, 2007; Revised Manuscript Received October 21, 2007

ABSTRACT

One-dimensional (1D) conductive nanowire is one of the most important components for the development of nanosized electronic devices, sensors, and energy storage units. Great progresses have been made to prepare the 1D-conducting polymeric nanofibers by the low concentration process or the synthesis with hard or soft templates. However, it still remains as a great challenge to prepare polymeric nanofibers with narrow dispersity, high aspect ratio, and good processibility. With the rod-like tobacco mosaic virus as the template, 1D-conducting polyaniline and polypyrrole nanowires can be readily prepared via a hierarchical assembly process. This synthesis discloses a unique way to produce composite fibrillar materials with controlled morphology and great processibility, which can promote many potential applications including electronics, optics, sensing, and biomedical engineering.

Self-assembled proteins, such as plant viruses and other bionanoparticles, exhibit fascinating structural features and sophisticated chemistries, which are advantageous characteristics for the development of novel nanoscale materials.[1−8] For instance, the native tobacco mosaic virus (TMV) particle possesses a unique tubelike structure and distinctive physiochemical properties that have made this system a robust and attractive platform for the deposition of inorganic materials on either the interior or the exterior surface to form one-dimensional (1D) nanostructures.[9−13] The virus is assembled from 2130 identical coat proteins arranged helically around a single strand of RNA. The entire particle measures 300 nm in length and 18 nm in diameter, and can be isolated from infected tobacco plants in gram quantities with relative ease. The virion remains intact at temperatures up to 60 °C and at pH values between 2 and 10.[14] Moreover, recent studies have shown that the surface properties of TMV can be chemically or genetically manipulated without interfering the integrity and morphology of virus.[1,15,16] Evidently, TMV-based materials have already shown great potential in nanoelectronics.[8,17]

On the other hand, polyaniline (PANi) and other conductive polymers has been extensively studied for optical and electronic applications.[18−20] Many practical syntheses of 1D nanostructured PANi have been developed.[21−26] However, preparation of conductive PANi nanowires with controllable morphologies and sizes, especially with good processibility, is still a challenge. In this letter, we demonstrate the fabrication of water-dispersible, conductive PANi nanowires using TMV as a template. Furthermore, much longer conductive PANi/TMV nanowires (>300 nm, greater than the length of a native TMV particle) can also be formed by a hierarchical assembly process.[27−29]

As shown in Scheme 1, conductive polyaniline/TMV composite nanowires can be readily prepared by incubation of TMV, aniline, poly(sulfonated styrene) (PSS), and ammonium persulfate (APS) at room temperature. Highly negative-charged PSS is used here both as the dopant acid to enhance the conductivity of PANi and to improve the stability of composite fibers in aqueous solution. As shown in Figure 1, a green transparent solution of PANi/TMV composites were observed after a 24 h reaction at pH 4, indicating the formation of the emeraldine form of PANi. The color of the reaction mixture changed to yellow at pH 5.0. We attribute the color change to the formation of branched poly or oligo-anilines at higher reaction pH.

* Corresponding authors. E-mail: (Q.W.) wang@mail.chem.sc.edu; (G.K.) koley@engr.sc.edu.
[†] Department of Chemistry and Biochemistry and Nanocenter.
[‡] Department of Electrical Engineering.
[§] The Electron Microscopy Centre.

10.1021/nl072134h CCC: $37.00
Published on Web 11/17/2007

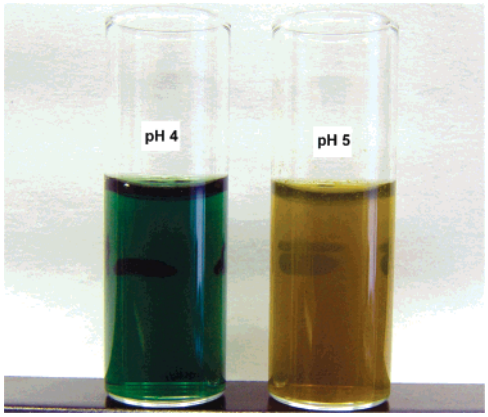

Figure 1. Optical image of PSS/PANi/TMV composite fibers in aqueous solution at pH 4.0 and 5.0. The concentrations of TMV templates are 1.0 mg/mL.

Scheme 1

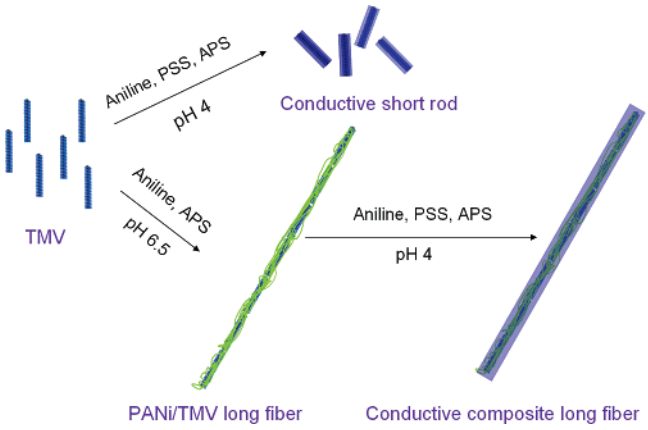

As shown in Figure 2a, the diameter of native TMV is around 18 nm. After negative staining with 2% uranium acetate, the 4 nm inner channel can be clearly visualized (Figure 2a, inset). Upon coating with PANi/PSS at pH 5.0, the diameter of composite nanowires was measured as 22 nm (Figure 2b). The inner channel could not be detected even after negative staining (Figure 2b, inset). The length of most nanowires is ~300 nm, which is similar to those of native TMV. Similarly, the PSS/PANi/TMV nanowires formed at pH 4.0 showed an increased diameter of ~26 nm while the length remained very similar to native TMV particles (Figure 2c). As shown in Figure 3, the peak at 260 nm of the UV−vis absorbance of all the samples is attributed to the absorbance of TMV (see the black line for the UV−vis spectra of native TMV). For the reaction conducted at pH 5.0, thorough dialysis against deionized water gave a PSS/PANi/TMV composite sample with two absorption peaks (ca. 260 and 427 nm) (blue line). The peak around 260 nm is attributed to the absorbance of TMV, and the peak at 427 nm attributed to oligoaniline in its branch form, which explains its nonconductive nature.[27,30] At pH 4.0, in addition to absorption at 260 nm, which is attributed to the absorbance of TMV, three absorption bands are observed that are consistent with the emeraldine salt form of PANI. Two absorption peaks at about 420 and 823 nm are attributed to polaron band transitions, and one peak at 320 nm is due to π-π^* transition of the benzenoid rings (purple line).[30] These peaks indicate that PANi is in its conducting form, which is similar to that obtained by either chemical or electrochemical methods.

To generate longer nanowires, we first synthesized long 1D composite nanofibers by treating TMV with a dilute solution of aniline and APS at near neutral pH. The formation of highly branched PANi at neutral reaction pH prevents lateral association of single PANi/TMV nanofibers (denoted as PANi/TMV/LF) due to the increase of steric repulsion (Figure 2d).[27] Such nanofibers exhibit homogeneous diameter and high aspect ratio, but no conductivity due to the branched structures of PANI. When preformed PANi/TMV/LF was treated with PSS, aniline, and APS at pH 4.0 or 5.0 (Scheme 1), long 1D fibers (denoted as PSS/PANi/LF) were produced with increased diameters (Figure 2e and 2f). The length of PSS/TMV/LF composite long fiber reached several micrometers. Unlike most reported syntheses of conducting polyaniline nanofibers that can only produce interconnected, branched fiber-networks or fiber-bundles, the PSS/PANi/LF synthesized by our method are predominantly individual fibers. Moreover, the PSS/PANi/LF can be easily dispersed in a dilute water solution or dispersed on solid surfaces by a simple spin-coating operation. If the reaction is conducted via a one-step process using aniline, APS, and TMV without PSS at pH 4.0, only a bundlelike structure can be obtained.[28] Clearly, highly negative-charged PSS acts not only as a dopant acid for the PANi to make them water-soluble and conductive, but also a highly charged outer cover to prohibit the aggregation of the composite nanofibers. Again, UV absorbance of PSS/PANi/LF at ~825 nm indicates the formation of conductive PANi on the nanofibers (Figure 3, green line).

Another well-known conducting polymer, polypyrrole (PPy), can also be used to coat TMV to afford 1D structure. At pH 3.6, the PPy-TMV composite nanowires (denoted as PSS/PPy/TMV) can be formed by incubating the pyrrole, PSS, APS, and TMV at room temperature for 24 h. As shown in Figure 4 (left), most of composite rods maintain the similar morphology as the native TMV. However, the diameter of PSS/PPy/TMV increased to about 22 nm after the reaction. When PANI/TMV/LF was employed as the template, the conductive PPy composite fibers (PSS/PPy/LF) could be prepared as its PANi analogues. As shown in Figure 4 (right), TEM gives the length of PSS/PPy/LF that can reach several micrometers, which is similar with its original template as shown in Figure 2d. The diameter of PPy composite fiber is about 28 nm (Figure 4, right inset).

TMV nanostructures have recently been characterized by Balandin and coauthors using piezoresponse force microscopy (PFM) yielding important information about the piezoelectric and flexoelectric properties.[31] However, PFM does not provide much information regarding the electrical conductivity of the NWs, which is intimately related to their applications as electronic and sensing devices. In our study, scanning spreading resistance microscopy (SSRM) was performed in conjunction with regular atomic force microscopy (contact mode) to obtain simultaneous electronic and

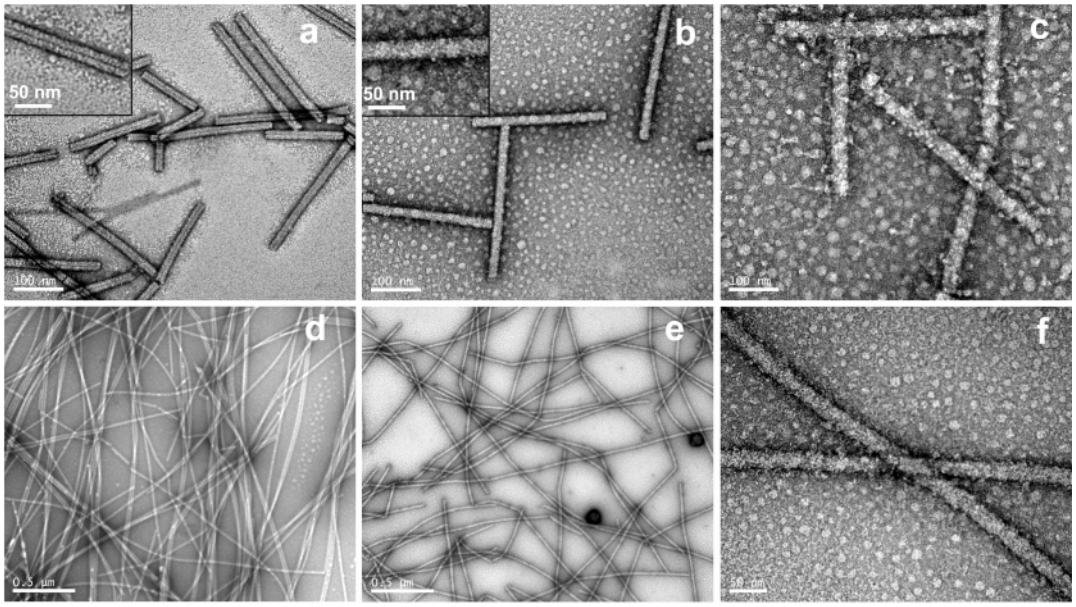

Figure 2. TEM images of (a) wt-TMV; (b) PSS/PANi/TMV nanowire from the pH 5.0 reaction; (c) PSS/PANi/TMV composite nanowire from the pH 4 reaction; (d) PANi/TMV long fiber (LF); (e) PSS/PANi/LF; and (f) an enlarged image of PSS/PANi/LF shows a average diameter of 28 nm.

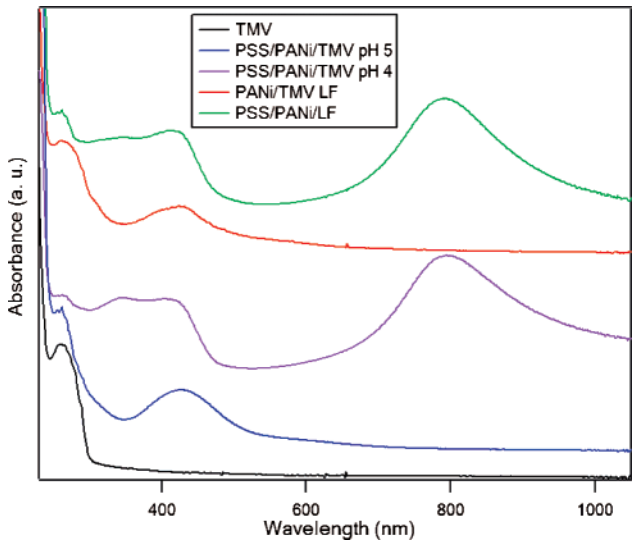

Figure 3. UV−vis spectra of native TMV and PANi/TMV composite fibers.

morphological information of the nanofibers. Schematic diagram of the SSRM measurement setup is shown in Figure 5a.[32]

The PSS/PANi/LF were dispersed on a doped silicon wafer ($\rho = 10$ ohm·cm) by casting 5 μL of 0.1 mg/mL composite fiber solution on the wafer and drying overnight at room temperature. To obtain reliable current imaging, a doped diamond-coated Si probe from Veeco metrology group (Veeco DDESP−FM) was used. However, the radius of these tips are rather large (i.e., ∼30−40 nm), which resulted in the diameter of the nanofibers in the image being much larger than actual due to tip convolution effects (Full width at half-maximum height is ∼180 nm in Figure 5d). This has also been observed in our earlier studies on GaN nanowires.[33] The nanowire may also have flattened to some extent (which are much softer than the diamond coating) due to contact mode imaging, contributing to the increased diameter. Nevertheless, the height of the nanofibers is correctly measured and is usually ∼25 nm, which is in agreement with the TEM images in Figure 4b. Simultaneously measured morphology and probe current images are shown in Figure 5b,c, which correlate very well with each other. The current on the nanofibers was found to be much less compared to that on the bare Si surface due to added resistance of the nanowire and a change in surface barrier between the nanowire and Si. However, because the probe moves as it scans, only partial overlap with the nanowire is possible for most of the scan. This can lead to inaccurate measurements. For better estimation of the electrical properties, we performed stationary current−voltage ($I-V$) measurements on the nanofibers as well as on the bare Si wafer surface. Figure 5e compares these two currents. We observe that the current on the bare Si surface is much larger than that on the nanofiber. However, both the currents increase exponentially (in the voltage range that could be safely applied to the nanofiber), indicating that it is primarily controlled by a potential barrier, which is most likely the nanofiber/Si or the probe/Si barrier (this is also confirmed from our measurements on Au-coated glass substrate as discussed below). Because an accurate estimation of the spreading resistance of the nanofiber will require a linear $I-V$ relationship, we performed measurements on nanofibers spread out on an Au-coated glass substrate. This will reduce the surface barrier of the nanowire/substrate junction and help accurately measure the nanowire resistance. However, extreme care has to be taken to position the probe exactly on the nanofiber and not on the Au surface to avoid shorting out and destroying the tip due to very low metal resistance. The measured stationary current−voltage ($I-V$) characteristic is shown in Figure 5f, which shows almost linearly increasing

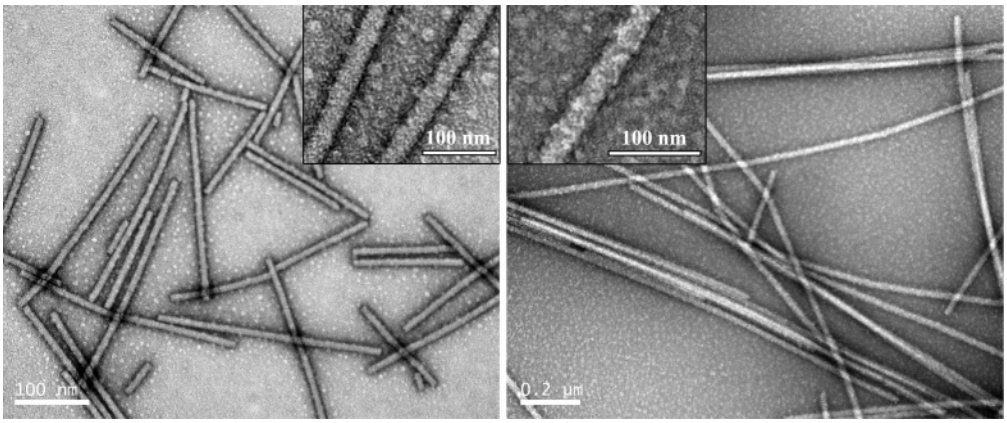

Figure 4. TEM images of PSS/PPy/TMV composite nanowires (left), and PSS/PPy/LF composite long fiber using pyrrole as starting materials (right).

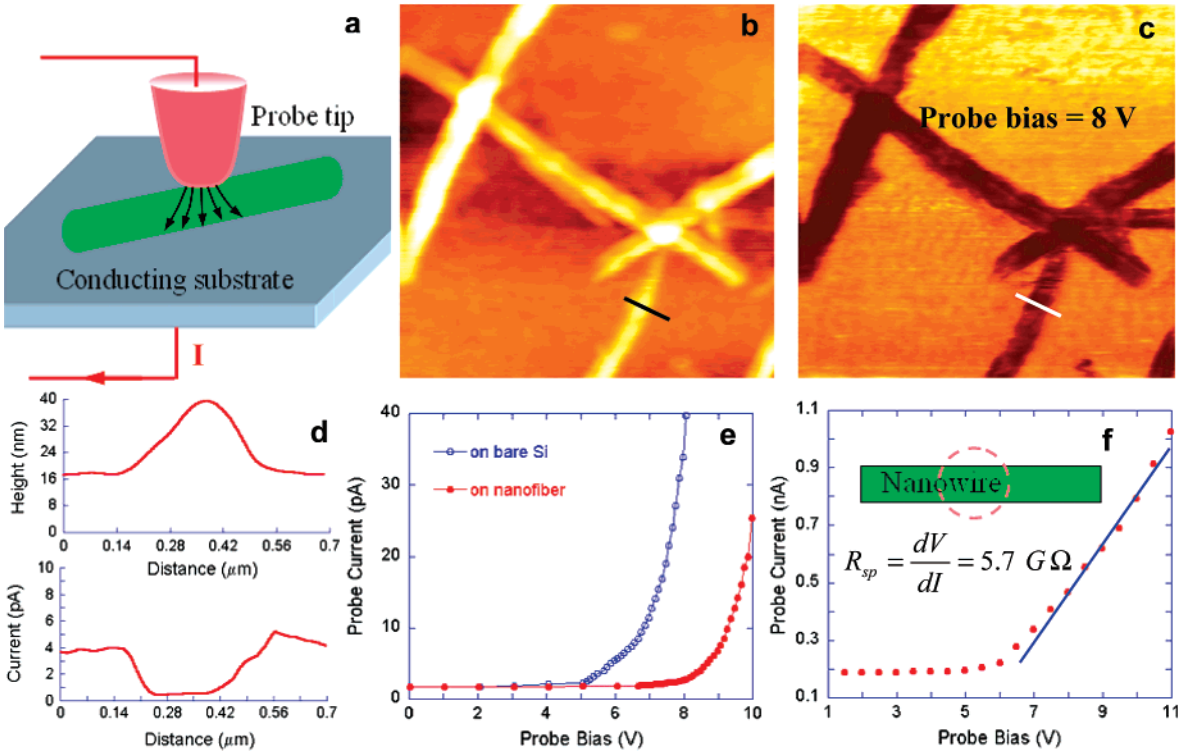

Figure 5. (a) Schematic diagram of the measurement set up. The sizes of tip and nanowire do not reflect the real setup. (b) 4 × 4 μm surface morphology image of PSS/PANi/LF composite nanowires on a Si wafer (scale bar is 60 nm). (c) Simultaneously obtained probe current map for the nanowires (scale bar is 10 pA). (d) Line-scans through the morphology and probe current images. (e) Stationary $I-V$ characteristics for the probe positioned on Si and on the nanowire. (f) Stationary $I-V$ characteristic for a nanofiber placed on an Au-coated glass substrate. Inset shows a schematic of the probe outline (shown by dotted circle) over the nanowire.

current for probe bias greater than 6 V. This is in contrast to Figure 5e, where an exponential rise in current was observed. In addition, the current is at least an order of magnitude larger than that measured on the nanofiber on Si for comparable bias. We believe this is due to lower probe/nanofiber barrier height for the Au substrate compared to the Si substrate. Another potential factor could be the native SiO_2 layer on the Si surface that can also significantly reduce the probe current in Figure 5e.

At higher biases, the $I-V$ characteristic of any rectifying junction is completely dominated by the diode series resistance. In the present case, the series resistance is mainly the nanowire-spreading resistance, because the resistance of the nanofiber/Au interface can be assumed to be negligible (due to a much larger contact area between the nanofiber and Au surface). The spreading resistance of the nanofiber can be estimated from slope dV/dI of the least-square fit line to the data points in the linear part of the $I-V$ curve in Figure 5f (the least-square fit to the data points is shown by the blue solid line). This comes out to be ~5.7 GΩ. For a hemispherical, indenting probe tip, the spreading resistance is related to the resistivity ρ as

$$R_{sp} = \frac{\rho}{(2\pi)r} = \frac{1}{(2\pi)r\sigma} \quad (1)$$

where r is the radius of nanofiber. Putting the value of R_{sp} and the probe radius (30 nm) in eq 1, the conductivity of the composite PSS/PANi/LF nanofiber is calculated as $0.93 \times 10^{-5}\ \Omega^{-1}\text{cm}^{-1}$. An alternate calculation of conductivity, neglecting any spreading of the current from the probe tip and only based on the resistance of the overlap area between the probe and the nanowire (see inset of Figure 5f for schematic geometry), can be obtained from the simple relation, $\sigma = l/RA$, from which σ can be calculated as $2.93 \times 10^{-5}\ \Omega^{-1}\text{cm}^{-1}$ (using $l = 25$ nm, $R = 5.7$ GΩ, and $A \approx 25 \times 60\ \text{nm}^2$). The important thing to note here is that both the methods are somewhat approximate, but the conductivity can be estimated to be on the order of low $10^{-5}\ \Omega^{-1}\text{cm}^{-1}$. Nevertheless, this represents the first conductivity measurements of TMV-based nanowires and is therefore significant by itself. This nanowire conductivity is not as high as those of semiconducting ones (few $\Omega^{-1}\text{cm}^{-1}$)[34] or carbon nanotubes ($1-5\ \Omega^{-1}\text{cm}^{-1}$),[35] but compares well with PANI nanofibers synthesized by other methods,[19,24] and would nonetheless permit useful applications in low-power electronic and sensor devices.

In conclusion, with native TMV as the template water-soluble, monodisperse conducting polymeric nanowires can be prepared via a hierarchical assembly and in situ polymerization process. Electronic properties measured using SSRM indicate a conductivity of $\sim 1 \times 10^{-5}\ \Omega^{-1}\text{cm}^{-1}$ for the composite PANI/TMV/LF nanofiber. This synthesis discloses a unique and versatile way to produce composite fibrillar materials with narrow dispersity, high aspect ratio, and high processibility, which can have many potential applications in electronics, optics, sensing, and biomedical engineering.

Acknowledgment. We thank Dr. S. Ghoshroy and J. Zhao for the help with the TEM measurements. This work was supported by NSF-DMR-0706431, the US DOD, and the W. M. Keck Foundation.

References

(1) Miller, R. A.; Presley, A. D.; Francis, M. B. *J. Am. Chem. Soc.* **2007**, *129*, 3104−3109.
(2) Holder, P. G.; Francis, M. B. *Angew. Chem., Int. Ed.* **2007**, *46*, 4370−4373.
(3) Lee, S.-W.; Mao, C.; Flynn, C. E.; Belcher, A. M. *Science* **2002**, *296*, 892−895.
(4) Flynn, C. E.; Lee, S.-W.; Peelle, B. R.; Belcher, A. M. *Acta Mater.* **2003**, *51*, 5867−5880.
(5) Mao, C.; Solis, D. J.; Reiss, B. D.; Kottmann, S. T.; Sweeney, R. Y.; Hayhurst, A.; Georgiou, G.; Iverson, B.; Belcher, A. M. *Science* **2004**, *303*, 213−217.
(6) Yoo, P. J.; Nam, K. T.; Qi, J.; Lee, S. K.; Park, J.; Belcher, A. M.; Hammond, P. T. *Nature Mater.* **2006**, *5*, 234−240.
(7) Wang, Q.; Lin, T.; Tang, L.; Johnson, J. E.; Finn, M. G. *Angew. Chem., Int. Ed.* **2002**, *41*, 459−462.
(8) Tseng, R. J.; Tsai, C.; Ma, L.; Ouyang, J.; Ozkan, C. S.; Yang, Y. *Nat. Nanotechnol.* **2006**, *1*, 72−77.
(9) Dujardin, E.; Peet, C.; Stubbs, G.; Culver, J. N.; Mann, S. *Nano Lett.* **2003**, *3*, 413−417.
(10) Fowler, C. E.; Shenton, W.; Stubbs, G.; Mann, S. *Adv. Mater.* **2001**, *13*, 1266−1269.
(11) Knez, M.; Bittner, A. M.; Boes, F.; Wege, C.; Jeske, H.; Maiss, E.; Kern, K. *Nano Lett.* **2003**, *3*, 1079−1082.
(12) Knez, M.; Sumser, M.; Bittner, A. M.; Wege, C.; Jeske, H.; Martin, T. P.; Kern, K. *Adv. Funct. Mater.* **2004**, *14*, 116−124.
(13) Balci, S.; Bittner, A. M.; Hahn, K.; Scheu, C.; Knez, M.; Kadri, A.; Wege, C.; Jeske, H.; Kern, K. *Electrochim. Acta* **2006**, *51*, 6251−6257.
(14) Shenton, W.; Douglas, T.; Young, M.; Stubbs, G.; Mann, S. *Adv. Mater.* **1999**, *11*, 253−256.
(15) Yi, H. M.; Nisar, S.; Lee, S. Y.; Powers, M. A.; Bentley, W. E.; Payne, G. F.; Ghodssi, R.; Rubloff, G. W.; Harris, M. T.; Culver, J. N. *Nano Lett.* **2005**, *5*, 1931−1936.
(16) Schlick, T. L.; Ding, Z. B.; Kovacs, E. W.; Francis, M. B. *J. Am. Chem. Soc.* **2005**, *127*, 3718−3723.
(17) Fonoberov, V. A.; Balandin, A. A. *Nano Lett.* **2005**, 5, 1920−1923.
(18) MacDiarmid, A. G. *Synth. Met.* **2002**, *125*, 11−22.
(19) Huang, J.; Kaner, R. B. *Chem. Commun.* **2006**, 367−376.
(20) Zhang, D. H.; Wang, Y. Y. *Mat. Sci. Eng., B* **2006**, *134*, 9−19.
(21) Huang, J.; Kaner, R. B. *J. Am. Chem. Soc.* **2004**, *126*, 851−855.
(22) Huang, J.; Virji, S.; Weiller, B. H.; Kaner, R. B. *J. Am. Chem. Soc.* **2003**, *125*, 314−315.
(23) Ma, Y. F.; Zhang, J. M.; Zhang, G. J.; He, H. X. *J. Am. Chem. Soc.* **2004**, *126*, 7097−7101.
(24) Chiou, N. R.; Lui, C. M.; Guan, J. J.; Lee, L. J.; Epstein, A. J. *Nat. Nanotechnol.* **2007**, *2*, 354−357.
(25) Ding, H. J.; Wan, M. X.; Wei, Y. *Adv. Mater.* **2007**, *19*, 465−269.
(26) Huang, J. X.; Kaner, R. B. *Angew. Chem., Int. Ed.* **2004**, *43*, 5817−5821.
(27) Niu, Z.; Bruckman, M. A.; Kotakadi, V. S.; He, J.; Emrick, T.; Russell, T. P.; Yang, L.; Wang, Q. *Chem. Commun.* **2006**, 3019−3021.
(28) Niu, Z.; Bruckman, M. A.; Li, S.; Lee, L. A.; Lee, B.; Pingali, S. V.; Thiyagarajan, P.; Wang, Q. *Langmuir* **2007**, *23*, 6719−6724.
(29) Bruckman, M. A.; Niu, Z.; Li, S.; Lee, L. A.; Varazo, K.; Nelson, T. L.; Lavigne, J. J.; Wang, Q. *NanoBiotechnology* **2007**, *3*, 31−39.
(30) Liu, W.; Kumar, J.; Tripathy, S.; Senecal, K. J.; Samuelson, L. *J. Am. Chem. Soc.* **1999**, *121*, 71−78.
(31) Kalinin, S. V.; Jesse, S.; Liu, W.; Balandin, A. A. *Appl. Phys. Lett.* **2006**, *88*, 153902.
(32) Koley, G.; Liu, J.; Mandal, K. C. *Appl. Phys. Lett.* **2007**, *90*, 102121.
(33) Koley, G.; Lakshmanan, L.; Wu, H.; Cha, H. Y. *Phys. Status Solidi* **2007**, *204*, 1123−1129.
(34) Cui, Y.; Wei, Q.; Park, H.; Lieber, C. M. *Science* **2001**, *293*, 1289−1292.
(35) Bachtold, A.; Hadley, P.; Nakanishi, T.; Dekker, C. *Science* **2001**, *294*, 1317−1320.

NL072134H